ELSEVIER

Journal of Molecular Catalysis A: Chemical 100 (1995) 1–11

JOURNAL OF MOLECULAR CATALYSIS A: CHEMICAL

The influence of metal oxides on the activity and selectivity of transition metal catalysts

Alexis T. Bell

Chemical Sciences Division, Lawrence Berkeley National Laboratory and Department of Chemical Engineering, University of California, Berkeley, CA 94720, USA

Received 1 June 1995; accepted 7 June 1995

Abstract

The catalytic activity and selectivity of transition metals are known to be affected by metal oxides deposited on their surface. Such deposits can result from the transfer of portions of the support during catalyst preparation or be introduced intentionally. The structure and composition of both monolayer and multilayer deposits of metal oxides on Rh and Pt are discussed and the effects of oxide composition and coverage on the rate of CO and CO_2 hydrogenation are examined. It is shown that the effectiveness of an oxide correlates with its Lewis acidity, and that the later property can be described by the Pauling electronegativity of the cations in the oxide. The effects of oxide deposits on other reactions are also reviewed.

Keywords: Activity; Metal oxides; Selectivity; Transition metal catalysts

1. Introduction

Transition metal catalysts are usually dispersed as small particles onto an oxide support in order to achieve a high metal surface area. Extensive studies conducted over the past twenty five years have shown that the composition of the support can affect the activity of the metal by as much as an order of magnitude, or even more in some cases (e.g., [1–5]). While subsequent analyses have revealed that some of the observed differences can be attributed to differences in metal dispersion, strong evidence remains for substantial influences of support composition on metal activity and selectivity. The origin of these effects has been the subject of considerable discussion in the literature. In the earliest attempts to provide an explanation, Schwab [6] and Solymosi [7] proposed that the metal oxide altered the electronic properties of the metal. While this hypothesis was soundly based on the principles of metal/semiconductor interfaces, subsequent experimental data revealed no evidence for a change in the bulk electronic properties of the metal due to the presence of metal/metal oxide contacts (see for example [5]). This led to the proposal, first articulated by Burch and Flambard [8], that highly active sites occur in the metal/metal oxide interfacial region. These sites were envisioned to be cations or anionic vacancies present at the edge of the metal oxide moieties. To explain the observed enhancement in the rate of CO hydrogenation over transition metals due to metal oxides, the authors proposed that activation of the C=O bond occurs via interaction of the oxygen end of a carbonyl group with the cation site. In later work, Sachtler

SSDI 1381-1169(95)00132-8

and coworkers [9,10], suggested that the nature of the interaction between the carbonyl group and the exposed cation at the edge of the oxide moieties might be similar to that of Lewis acid–base complexes formed in solution between carbonyl ligands in metallocarbonyl complexes and Lewis acids such as $AlCl_3$.

In this paper we will summarize studies conducted in our laboratory aimed at developing a more quantitative description of the effects of metal oxides on the activity and selectivity of transition metals. Results will be presented for both planar, model systems consisting of a metal foil decorated with controlled quantities of metal oxide and for dispersed metal catalysts. While most of the discussion will focus on the hydrogenation of CO and CO_2, recent investigation of other reaction systems will be reviewed as well.

2. Planar model systems

Metal foil or single crystal decorated with controlled amounts of the oxide exhibit catalytic activities and selectivities that are essentially identical to those metal oxide-supported metal catalysts, but are more amenable to control of the oxide coverage, and characterization of the oxide composition by various surface analytical techniques [11–24]. We have used this approach to investigate the structure of the oxide and its bonding to the underlying metal, and to determine the effects of oxide composition and coverage on the activity of Rh for the hydrogenation of CO and CO_2.

Sample preparation and characterization and subsequent reaction studies is performed in an UHV chamber equipped with a cylindrical mirror analyzer for Auger electron spectroscopy, a quadrupole mass spectrometer for gas analysis, and a high-pressure isolation cell for conducting reaction studies [20,21,23]. The reaction cell is connected to a gas recirculation loop. Reactant gases are introduced into the recirculation loop from a gas manifold and the contents of the loop are recirculated by means of a metal bellows pump. The composition of the recirculated gas is determined by gas chromatography. A second UHV chamber, equipped with a sample preparation chamber, is used to characterize the deposited metal oxide by XPS [23].

A 1 cm^2 foil of Rh or Pt is mounted on a manipulator. Prior to the initiation of reaction, the foil is cleaned by high-temperature annealing and sputtering to remove boron and sulfur contamination. Metal oxide is deposited by evaporating the desired metal in a background of 10^{-7} Torr of O_2. After deposition the sample is oxidized in 10^{-6} Torr of O_2 at 623 K for 5 min. To remove oxygen adsorbed on the surface of the foil, 10^{-7} Torr of CO is admitted to the chamber for 20 s, and the sample is then flashed to 673 K.

The amount of metal oxide deposited on to the foil can be determined from either AES, XPS, ISS, or CO chemisorption experiments [23,25]. All three techniques indicate that titania grows on the surface of Rh according to a Stranski–Krastanov model. For example, deposition of submonolayer quantities of titania on either Rh foil or a Pt(111) surface produces a monolayer thick film. As the deposition proceeds, the intensity of the Rh signal observed by AES, XPS, or ISS decreases linearly, as does the amount of CO adsorbed on the exposed metal surface. Close to the point where the first monolayer nears completion, there is evidence of some three-dimensional film growth prior to initiation of the formation of a second monolayer.

LEED characterization of titania overlayers reveals that both monolayer and multilayer films are amorphous, if not annealed at temperatures in excess of 773 K [26]. Fig. 1 shows that the total XPS signal for Ti ($Ti^{4+} + Ti^{3+}$) increases with increasing titania coverage; however the signal for Ti^{3+} rises to a maximum at 1.0 ML and then decreases. From the angular dependence of the Ti^{3+} signal relative to the Ti^{4+} signal it is deduced that the Ti^{3+} is concentrated at the interface between the oxide layer and the Pt(111) substrate. A model based on this interpretation of the metal oxide structure and bonding to the underlying metal properly describes the observed decrease of the Ti^{3+} signal with increasing coverages above

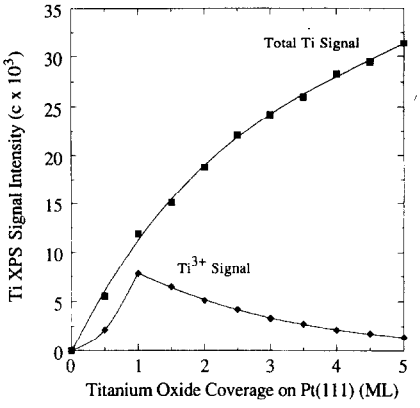

Fig. 1. Total Ti XPS signal ($Ti^{4+} + Ti^{3+}$) from titanium oxide deposits on Pt(111) and the Ti^{3+} component plotted as a function of coverage. After each successive 0.5 ML deposition the surface was annealed in 1×10^{-6} Torr O_2 at 300°C. (Reproduced with permission from ref. [26].)

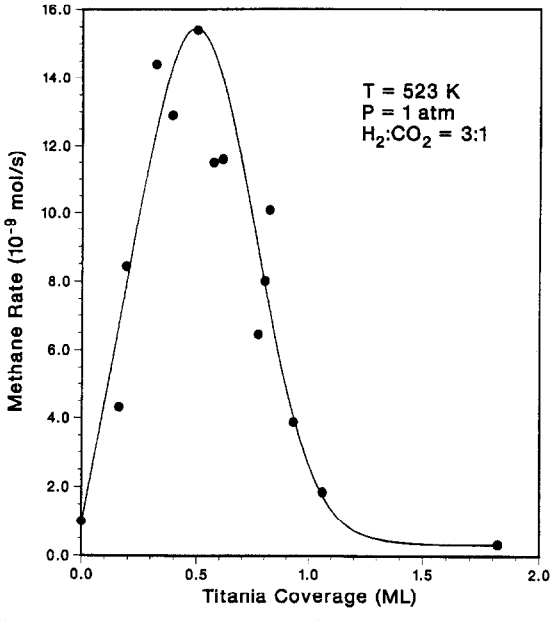

Fig. 2. The rate of methane formation from CO_2 hydrogenation over a Rh foil plotted as a function of titania coverage ($H_2/CO_2 = 3$, $P = 1$ atm, and $T = 523$ K). (Reproduced with permission from ref. [20].)

1.0 ML. These results suggest that the titania overlayer bonds to the Pt surface in such a fashion that electron transfer occurs from the Pt to the Ti cation in the first layer of the oxide. Second and subsequent layers more nearly resemble TiO_2. A similar mode of bonding is also expected for titania deposited on Rh.

The effects of submonolayers deposits of titania on the catalytic activity of Rh for the hydrogenation of CO_2 to methane is illustrated in Fig. 2 [24]. For titania coverages below 0.5 ML the rate of methane formation rises, reaching a maximum value that is nearly 16 times that for clean Rh. Above a coverage of 0.5 ML, the rate of methane formation decreases and eventually falls below that for clean Rh. A similar pattern has been observed for the effects of titania deposits on the hydrogenation of CO to methane; however, in this case, the maximum degree of rate enhancement is 2.8–3.0 [11]. We have recently reported that effects similar to those for titania are observed for tantala, niobia, vanadia, tungstena, and iron oxide [23,24]. For each oxide the maximum in catalytic activity for CO or CO_2 hydrogenation occurs at about 0.5 ML, but as indicated in Table 1 the maximum enhancement in the rate of methane formation is a function of oxide composition [23,24].

To interpret the effects of metal oxide composition and coverage, it is useful to review what is known about the mechanisms of CO and CO_2 hydrogenation. Since most of our results are for Rh, this discussion will be restricted to this metal. For the case of CO hydrogenation, studies by Sachtler and Ichikawa [9] suggest that the rate limiting step in the formation of methane is the rupture of the C–O bond. Hydrogenation of chemisorbed CO on Rh/SiO_2 produces CO and H_2O concurrently. Promotion of the Rh with titania or mangana reduces the peak temperature for the for-

Table 1
Maximum rate enhancement for methane formation from CO and CO_2 by 0.5 ML metal oxide deposits on Rh foil (reproduced with permission from ref. [24].)

CO_2 hydrogenation [a]		CO hydrogenation [b]	
Oxide	Max. rate enhancement	Oxide	Max. rate enhancement
TiO_x	15	TaO_x	3.9
NbO_x	13	TiO_x	3.0
TaO_x	12	NbO_x	2.5
ZrO_x	5.4	–	–
VO_x	5.1	VO_x	2.1
WO_x	5.0	WO_x	2.1
FeO_x	0.0	FeO_x	1.7

[a] $H_2/CO = 3$, $P = 1$ atm, $T = 523$ K.
[b] $H_2/CO_2 = 2$, $P = 1$ atm, $T = 553$ K.

1a. $CO_{2,g} + 2S \rightleftharpoons CO_s + O_s$

1b. $CO_g + S \rightleftharpoons CO_s$

2. $H_{2,g} + 2S \rightleftharpoons 2H_s$

3. $2H_s + CO_s \rightleftharpoons H_2CO_s + 2S$

4. $H_2CO_s + S \rightarrow CH_{2,s} + O_s$

5. $O_s + H_s \rightleftharpoons OH_s$

6. $OH_s + H_s \rightarrow H_2O_g$

7. $CH_{2,s} + H_s \rightleftharpoons CH_{3,s}$

8. $CH_{3,s} + H_s \rightarrow CH_{4,s}$

Fig. 3. Proposed mechanism for CO and CO_2 hydrogenation over Rh.

mation of both products by the same degree. However, since the hydrogenation of CO occurs at a lower temperature than that required for the dissociation of CO in the absence of H_2, suggesting the cleavage of the C–O bond is from an H_xCO species. Mori et al. [27–29] and Rieck and Bell [30] arrive at a similar conclusion from experimental observations. Theoretical support for the involvement of an H_xCO species in the rate limiting step is also provided by BOC–MP (bond order conservation–Morse potential) calculations reported by Shustorovich and Bell [31]. A plausible mechanism for the hydrogenation of CO on metallic Rh is shown in Fig. 3. As discussed below, this scheme leads to reaction kinetics that are consistent with those observed experimentally.

The hydrogenation of CO_2 over Group VIII metals is thought to proceed via the dissociative adsorption of CO_2 to form CO_s and O_s, whereafter the adsorbed CO undergoes hydrogenation according to the scheme shown in Fig. 3. This mechanism of CO_2 hydrogenation is supported by the studies of Amariglio et al. [32] on Rh powder. Following room-temperature adsorption of CO_2, the passage of H_2 over the catalyst produced H_2O in the amount of one molecule of H_2O for every molecule of CO_2 adsorbed. TPR of the residually adsorbed CO resulted in the formation of CH_4 and H_2O in a 1:1 ratio with identical peak temperatures, suggesting that, as in the case of CO hydrogenation, rupture of the C–O bond in a species such as H_2CO_s is the rate-limiting step. More recently, Fisher and Bell [33] have reported in situ infrared observations and rate measurements supporting this interpretation of CO_2 hydrogenation over Rh. Steps 1–8 represent a mechanism for CO_2 hydrogenation which is consistent with the reported experimental observations.

As noted earlier, it has been proposed that the interaction between the oxygen end of adsorbed CO or H_2CO and cations of the metal oxide can be thought of as a Lewis acid–base interaction, viz., $H_2CO \rightarrow Ti^{3+}$. If this hypothesis is correct, then the degree of rate enhancement for CO and CO_2 hydrogenation should correlate with the Lewis acidity of the metal cation in the oxide. As a measure of Lewis acidity, one can take the Pauling electronegativity, since Lewis acidity is proportional to the cation electronegativity [34,35]. Fig. 4 shows a strong correlation between the maximum rate of CO_2 hydrogenation and the Pauling electronegativity which is determined by from the expression

$$\chi_i = \chi_o(1 + 2Z) \quad (1)$$

In Eq. 1 χ_i is the electronegativity of the cation, χ_o is the electronegativity of the element (Pauling scale), and Z is the oxidation state of the cation determined from XPS [23,36,37]. The correlation presented in Fig. 4 supports the hypothesis that Lewis acidity is the primary property determining

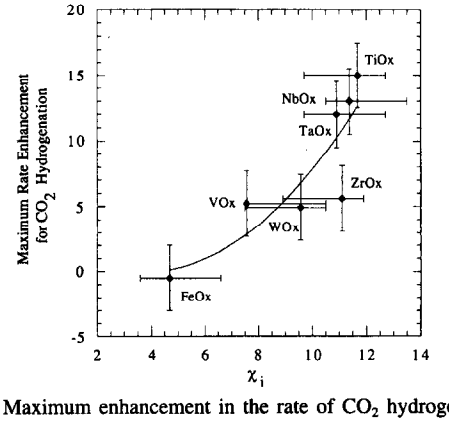

Fig. 4. Maximum enhancement in the rate of CO_2 hydrogenation plotted as a function of the average electronegativity of the metal cation in the oxide. (Reproduced with permission from ref. [23]).

promoter effectiveness. A further point of note is that the proposed interpretation aptly explains why the activity of for CO hydrogenation over supported Rh increases in the following order of support composition $Nb_2O_5 > ZrO_2 > SiO_2 \approx MgO$ [38,39].

The metal cations involved in promotion of CO and CO_2 hydrogenation are those located at the boundary between the metal oxide deposit and the underlying metal. Evidence from XPS [20] and STM [40] suggest that at submonolayer coverages titania covers the surface in the form of islands. Monte Carlo simulations of the growth of the overlayer show that with increasing metal oxide coverage the surface concentration of cation sites located at the perimeter of the oxide overlayer passes through a maximum at about 0.5 ML, independent of the number of nucleations sites assumed. This would explain why the maximum enhancement in the rates of CO and CO_2 hydrogenation always occur at a metal oxide coverage of about 0.5 ML (see Fig. 2, for example).

3. Dispersed metals

Supported metal catalysts are most often prepared by either incipient wetness or ion exchange techniques. During preparation and subsequent reduction, decoration or even partial encapsulation of the supported metal particles can occur [1–5]. In the former case, dissolution of a small portion of the support and subsequent precipitation of the dissolved material together with the metal precursor during drying results in the deposition of oxide over the newly formed metal particles. The extent to which oxide deposition occurs depends on both the solubility of the oxide and the pH of the precursor solution. Coverage of the metal particles can also occur due to migration of oxide or suboxide species during reduction of the catalyst. In this case the extent of migration depends on the relationship of the reduction temperature to the Tammann temperature of the oxide or suboxide; the closer the reduction temperature is to the Tammann temperature, the more likely that oxidic species will migrate onto the dispersed metal particles. Since the suboxides of a given metal oxide exhibit a lower surface tension than the oxide, suboxide moieties will wet the metal particles more effectively than will oxide moieties.

We have conducted a thorough investigation of the decoration of Ru particles supported on titania in which the extent of particle decoration could be determined by combining the results of characterization by TEM and ^1H NMR [41–43]. Titania-supported Ru catalysts were prepared by incipient wetness impregnation of TiO_2 with an aqueous solution of $Ru(NO)(NO_3)_3$. The impregnated titania was air dried at 383 K for 16 h and then reduced at 473 K in a flow of H_2.

For TEM observation, the catalyst is dry dispersed onto carbon-coated copper grids. Micrographs were obtained on a Topcon 002B transmission electron microscope operated at 200 kV, with a nominal point-to-point resolution of 1.9 Å. Ru particles are identified by using a combination of selected area diffraction techniques and measurement of lateral fringe spacings.

^1H NMR measurements are performed on a home-built spectrometer operating at 250 MHz. An in situ NMR probe was attached to a volumetric adsorption apparatus to allow for the collection of NMR spectra at various temperatures and adsorbate pressures. Typically, 500 transients are averaged for each spectrum, using a delay of 0.3 s, which is sufficient to avoid saturation of the resonance corresponding to hydrogen on metal.

Fig. 5 and Fig. 6 show high-resolution TEM micrographs of Ru/TiO_2 taken after reduction at 573 and 773 K, respectively [41]. Ruthenium particles with varying amounts of oxide overlayer encapsulation (fully, partially, and unencapsulated) are observed after reduction at 573 K. Unencapsulated Ru particles with clearly exposed faceted surfaces are shown in Fig. 5a, whereas partially and fully encapsulated particles are shown in Fig. 5b. Reduction at 773 K results in the disappearance of any unencapsulated Ru particles. Only partially and totally encapsulated Ru particles are now observed. In Fig. 6a, a large par-

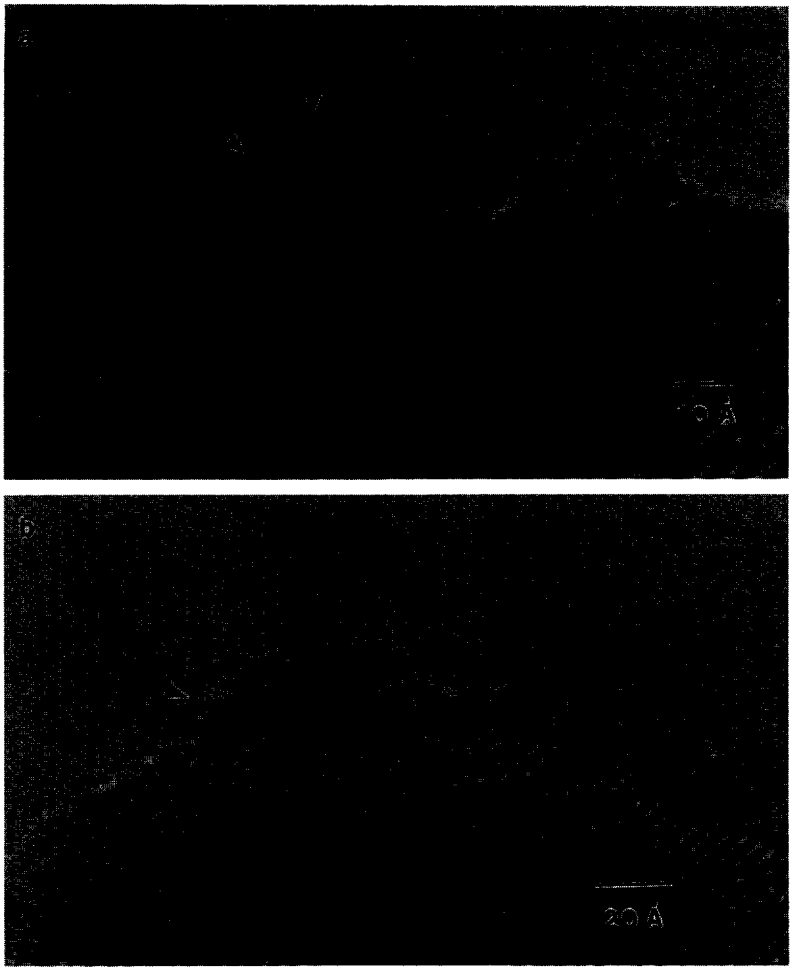

Fig. 5. Micrographs of titania-supported Ru particles ($Ru/TiO_2(A)$) after reduction at 573 K. In Fig. 5a, the faceted (001) and (101) surfaces of the Ru particles are clearly exposed. In Fig. 5b, the Ru particles are encapsulated by an amorphous overlayer, indicated by the hollow arrow. Only a small portion of one Ru particle surface is partially exposed (black arrow). (Reproduced with permission from ref. [41].)

ticle with approximately 30% of its surface exposed is shown. In Fig. 6b, a thin (7–8 Å) amorphous layer is observed to encapsulate the Ru particles. Estimation of the Ru particle size from an analysis of approximately 100 particles reveals that the reduction temperature has no effect on the average particle size for reduction temperatures between 473 and 773 K.

^1H NMR spectra taken after reduction of $Ru/TiO_2(A)$ and subsequent 10 min exposure to 400 Torr of H_2 at 373 K are presented in Fig. 7a [41]. Two peaks are now observed – one at 3 ppm due to hydroxyl groups on the support and the second at -53 to -64 ppm due to hydrogen adsorbed on Ru[44,45]. For each reduction temperature, the intensity of the 3 ppm peak seen in Fig. 7a is larger than that measured prior to hydrogen dosage, indicating that some of the absorbed H_2 has spilled onto the TiO_2. ^1H spectra taken after evacuation (10^{-5} Torr) of the reversibly adsorbed H_2 at 300 K for 10 min are shown in Fig. 7b.

Quantitative estimates of hydrogen uptake on the catalyst surfaces were obtained by comparing the integrated intensities from the NMR spectra with those of a reference sample. The moles of hydrogen adsorbed at a pressure of 400 Torr are designated H_{Ru}, H_{TiO_2}, and H_{total}. Similarly, the moles of hydrogen adsorbed irreversibly are designated $H_{i,Ru}$, H_{TiO_2}, and $H_{i,total}$. The amount of hydrogen adsorbed irreversibly on Ru was

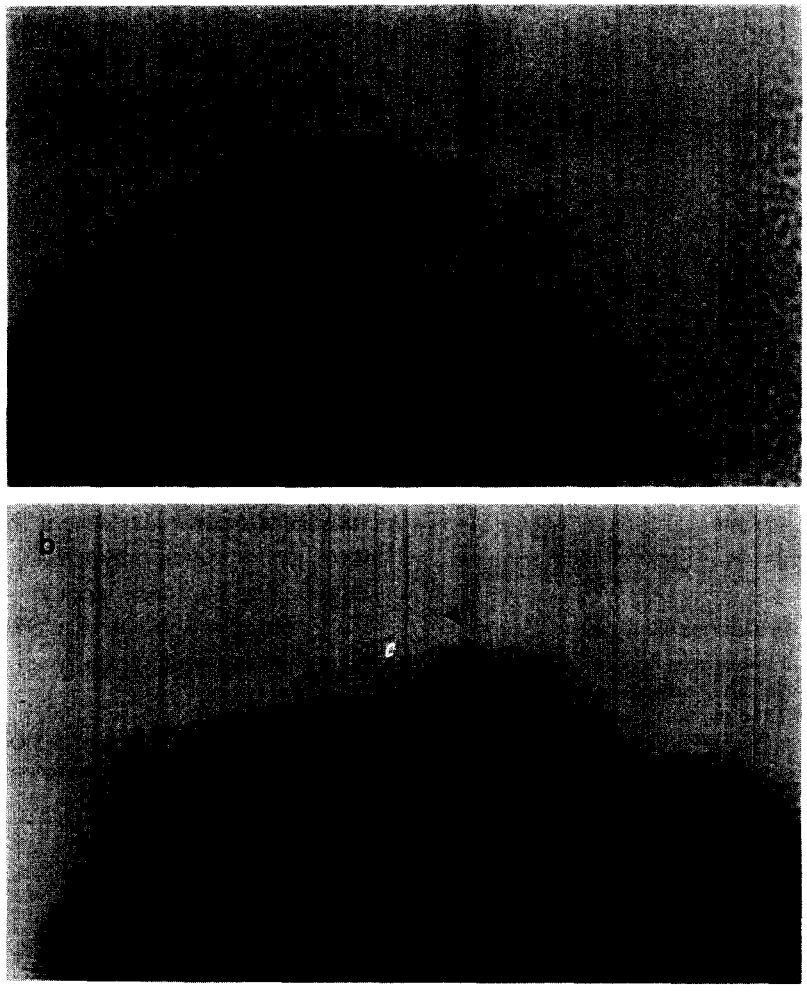

Fig. 6. Micrographs of titania-supported Ru particles ($Ru/TiO_2(A)$) after reduction at 773 K. In Fig. 6a, the Ru particle (with $d_{100}=2.34$ Å fringes visible) is partially encapsulated by an amorphous overlayer (hollow arrow), while a small portion of its surface is exposed (black arrow). In Fig. 6b, the Ru particles are completely encapsulated by an amorphous overlayer, indicated by the black arrow. (Reproduced with permission from ref. [41].)

obtained by integration of the upfield peak in Fig. 7b, whereas the amount of irreversibly adsorbed hydrogen on the support due to spillover was determined by comparing the integrated intensities of the peak at 3 ppm for samples evacuated before and after exposure to hydrogen.

The ratio of $H_{i,Ru}$ and $H_{i,total}$ to the total moles of Ru in the sample of $Ru/TiO_2(A)$, Ru_{total}, is plotted in Fig. 8 as a function of the reduction temperature [41]. As the reduction temperature increases from 473 K to 773 K, the ratio of $H_{i,Ru}/Ru_{total}$ decreases from 0.33 to 0.11, and the ratio of $H_{i,total}/Ru_{total}$ decreases from 0.54 to 0.12. The difference between these two ratios at each reduction temperature is an estimate of the amount of hydrogen spilled over onto the support. It is evident that hydrogen spillover is significant when the catalyst is reduced at 473 K and decreases monotonically to zero as the reduction temperature is raised to 773 K.

Since the size of the Ru particles in $Ru/TiO_2(A)$ does not change with increasing reduction temperature (see above), the decrease in the ratio of $H_{i,Ru}/Ru_{total}$ seen in Fig. 8 can be attributed to the progressive coverage of Ru particles by an overlayer of TiO_x. As noted above, TEM micrographs of $Ru/TiO_2(A)$ taken after reduction at 773 K clearly show evidence of an amor-

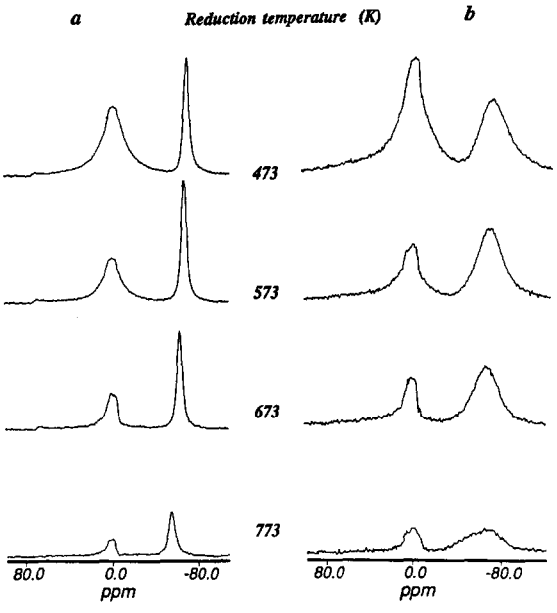

Fig. 7. ^{1}H NMR spectra of hydrogen on $Ru/TiO_2(A)$ as a function of the reduction temperature. The resonance lines near 0 ppm are ascribed to hydrogen on TiO_2, and the resonance lines near −60 ppm) are ascribed to hydrogen on Ru. Column (a) shows spectra obtained at 373 K and a H_2 pressure of 400 Torr. Column (b) shows spectra obtained at 300 K after 10 min evacuation. The spectra in columns (a) and (b) are plotted using two different intensity scales, each normalized relative to the upper spectrum. (Reproduced with permission from ref. [41].)

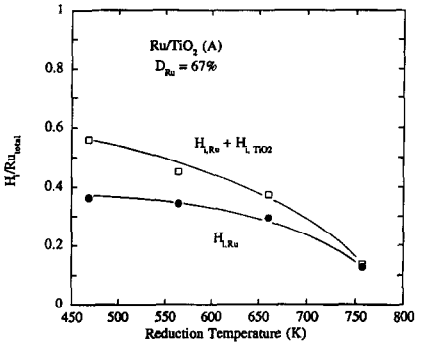

Fig. 8. The effect of the reduction temperature on the irreversible chemisorption of hydrogen on Ru and TiO_2 for $Ru/TiO_2(A)$. (Reproduced with permission from ref. [41].)

phous TiO_x layer on the surface of the Ru particles. Similar overlayers have previously been observed by TEM for Rh/TiO_2 reduced at elevated temperatures [46,47]. A measure of the fraction of the Ru particle surface available for H_2 chemisorption can be determined by combining the results obtained from TEM and ^{1}H NMR. The Ru dispersion obtained from TEM is equal to Ru_{surf}/Ru_{total}, the ratio of Ru atoms at the surface of the particle to the total Ru atoms in the particle. If it is assumed that $H_{i,Ru}/Ru_{exp} = 1$, where Ru_{exp} is the number of exposed Ru atoms in an average particle available for H_2 chemisorption, then the ratio of Ru_{exp}/Ru_{total} can be calculated from the ratio of $H_{i,Ru}/Ru_{total}$ determined by NMR (Table 2). It is evident that for $Ru/TiO_2(A)$ reduced at 573 K $Ru_{exp}/Ru_{surf} = 0.50$ and that the value of this ratio decreases to 0.15 when the reduction temperature is raised to 773 K. For $Ru/TiO_2(B)$ the value of $Ru_{exp}/Ru_{surf} = 0.15$ even when reduction is carried out at 573 K. This suggests that the smaller Ru particles present in $Ru/TiO_2(B)$ are more easily covered by a TiO_x overlayer than the larger Ru particles present in $Ru/TiO_2(A)$. $Ru_{exp}/Ru_{surf} = 0.96$ for Ru/SiO_2 reduced at 573 K, indicating that virtually all of the surface Ru

Table 2
Hydrogen uptake on Ru/TiO_2 and Ru/SiO_2 determined by ^{1}H NMR and volumetric chemisorption (reproduced with permission from ref. [41].)

Catalyst	$Ru/TiO_2(A)$	$Ru/TiO_2(B)$		Ru/SiO_2
Ru loading (wt%)	4.76	1.52		4.90
d_{TEM} (Å)	15	8		35
$D_{Ru} = Ru_{surf}/Ru_{total}$	0.67	1.00		0.28
Reduction temp. (K)	573	773	573	573
^{1}H NMR measurement				
H_{total}/Ru_{total} [f]	0.63	0.17	1.10	-
H_{Ru}/Ru_{total} [a]	0.33	0.15	0.38	0.48
$H_{TiO}2/Ru_{total}$ [a,f]	0.30	0.02	0.72	-
$H_{i,total}/Ru_{total}$ [e,f]	0.44	0.12	0.63	-
$H_{i,Ru}/Ru_{total}$ [e,b]	0.33	0.11	0.15	0.25
$Hi,TiO2/Ru_{total}$ [e,b,f]	0.11	0.11	0.47	-
Volumetric H_2 chemisorption				
H_{total}/Ru_{total} [c]	0.59	0.16	1.12	0.56
H_i/Ru_{total} [e]	0.39	-	0.70	-
H_i/Ru_{total} [d]	0.29	0.09	0.59	0.28

[a] H_{total}: Hydrogen uptake after H_2 adsorption at 373 K, 400 Torr H_2.
[b] H_i: Hydrogen uptake after evacuation (5×10^{-6} Torr) 10 min at 300 K.
[c] Hydrogen uptake after adsorption at 373 K.
[d] Hydrogen uptake after evacuation at 373 K.
[e] Hydrogen uptake after evacuation at 300 K.
[f] All values for H on TiO_2 obtained from NMR intensities may exhibit systematic deviations because T_1 relaxation times for H on TiO_2 are longer than for H on Ru.

Table 3
Characteristics of Na-containing and Na-free Ru/TiO_2 (reproduced with permission from ref. [41].)

Catalyst	Na-cont. Ru/TiO_2			Na-free Ru/TiO_2		
	A1	B1	C1	A2	B3	C2
Ru (wt%)	1.52	4.70	6.60	1.52	4.76	6.65
Na (wt%)	0.33	1.00	1.70	0.01	0.03	0.02
D_{Ru} [a]	0.83	0.70	0.56	0.77	0.67	0.50
$H_{i,Ru}/Ru_{total}$ [b]	0.14	0.07	0.05	0.38	0.34	0.28
θ_{TiO_x} [c]	0.83	0.90	0.91	0.51	0.49	0.44
$1-\theta_{TiO_x}$	0.17	0.10	0.09	0.49	0.51	0.56
Enhancement in TiO_x coverage due to Na	1.64	1.82	2.07	1.00	1.00	1.00

[a] Ru dispersion determined from TEM images.
[b] Hydrogen uptake determined by 1H NMR.
[c] $\theta_{TiO_x} = 1-[(H_{i,Ru}/Ru_{total}/D_{Ru}]$.

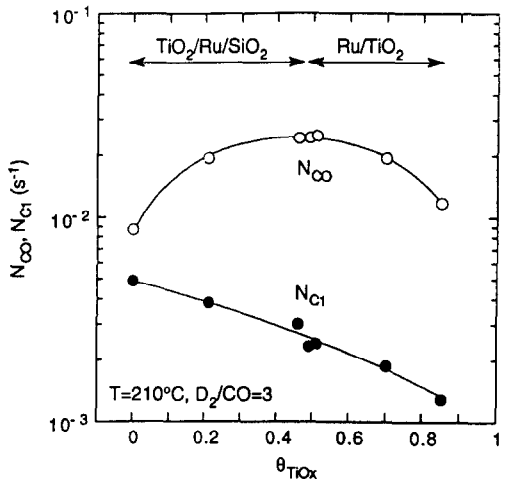

Fig. 9. Turnover frequencies for CO consumption, N_{CO}, and CH_4 formation, N_{C1}, as a function of TiO_x coverage. The turnover frequencies are based on Ru surface sites available for H_2 chemisorption. (Reproduced with permission from ref. [42].)

atoms are available for H_2 adsorption, consistent with the observation by TEM that all of the Ru particle surface is free.

If Na is present either as a contaminant in the precursor, or is added intentionally, the extent of coverage of the Ru particles by oxidic moieties increases as shown in Table 3 [43]. For a given catalyst, the degree of enhancement in the TiO_x coverage due to Na can be as much as a factor of two. TEM analysis of the Na-containing samples revealed the presence of various sodium titanate phases, $Na_xTi_yO_z$. Since the surface diffusion temperature (Tammann temperature) for sodium titanates are significantly lower than those for either anatase or rutile, a greater extent of surface diffusion is expected for sodium titanates than for the pure titania phase at a given reduction temperature.

The effects of titania coverage of the Ru on catalyst activity and selectivity for Fischer–Tropsch synthesis are illustrated in Figs. 9-11 [42]. To span the full range of titania coverages, both Ru/TiO_2 and TiO_2-promoted Ru/SiO_2 catalysts were used. The average particle size of the Ru particles for both catalysts was essentially the

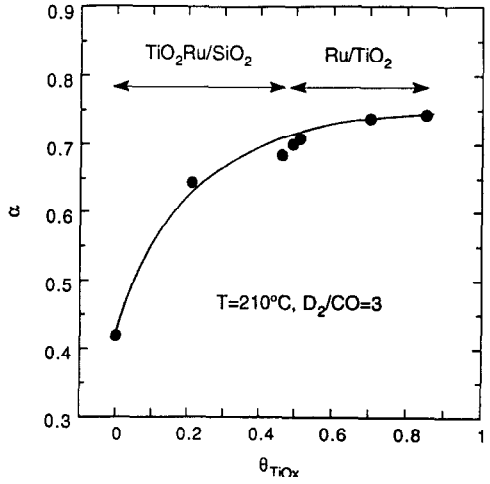

Fig. 10. The probability of chain growth, α, as a function of TiO_x coverage. (Reproduced with permission from ref. [42].)

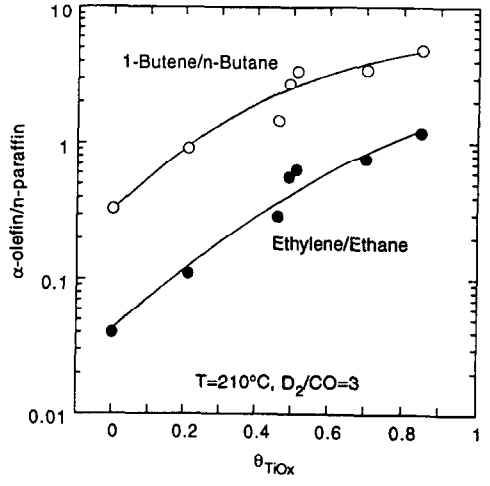

Fig. 11. The olefin to paraffin ratio for C_2 and C_4 products as a function of TiO_x coverage. (Reproduced with permission from ref. [42].)

same, so as to minimize the effects of particle size. Fig. 9 demonstrates that as the coverage by titania increases the turnover frequency for CO consumption passes through a maximum in a manner similar to that seen in Fig. 2 for metal oxide-promoted Rh foil. Titania coverage also has an effect on the probability of chain growth, α, and the olefin-to-paraffin ratio. As seen in Fig. 10 and Fig. 11, the value of α and the olefin-to-paraffin ratio increase monotonically with increasing titania coverage.

The maximum in the turnover frequency for CO hydrogenation observed at $\theta_{TiO_x} = 0.5$ is attributed to the occurrence of a maximum in the concentration of cation sites located at the perimeter of the oxide overlayer covering the Ru particles. Thus, as in the case of titania deposited on Rh foil, Ti^{3+} and Ti^{4+} cations present at the perimeter of the overlayer play a critical role in enhancing the rate of CO consumption. The decrease in methane formation with increasing θ_{TiO_x} is due in part to a reduction in the hydrogenolysis activity of Ru as more of the surface of the Ru particles is covered, and in part, to a decrease in the supply of adsorbed hydrogen. The latter trend also accounts for the increase in α and the olefin-to-paraffin ratio.

3.1. Effects of metal oxides on other reactions

As discussed in the preceding sections, metal oxides can significantly affect the activity and selectivity of transition metal catalysts for the hydrogenation of CO and CO_2. While other reaction systems have been examined less extensively, they are worthy of note. Studies of aldehyde and ketone hydrogenation have shown that the activity of transition metals for the hydrogenation of aldehydes and ketone are enhanced significantly when promoted with metal oxides, particularly titania [5,48–51]. In close similarity to what is observed for CO and CO_2 hydrogenation, the activity of Rh for acetone hydrogenation to isopropanol passes through a maximum at about 0.5 ML with increasing titania coverage [51]. The hydroformylation of ethylene over Rh also exhibits a maximum in the rate of propanaldehyde formation at a titania coverage of 0.5 ML [52] and studies conducted with silica-supported Rh [53] and Pd[54] show rate enhancement when the metal is promoted with ZnO or Nb_2O_5, respectively. Likewise, NO reduction by H_2 is found to proceed much more rapidly on titania-supported Rh and titania-promoted Rh supported on silica [55]. In each of the above examples, the increase in activity is attributed to interaction of the oxygen end of the reactant (i.e., CO or NO) with exposed cations of the oxide present at the boundary between the oxide and the metal. By contrast, investigation of ethylene hydrogenation and ethane hydrogenolysis show no beneficial effects of oxide promotion, but only a linear decrease in activity proportional to the extent to which the metal surface is covered [55]. These results suggest that when the reactant does not interact with the oxide, as well as the metal, a loss in catalytic activity occurs due to the reduction in exposed surface area of the metal.

4. Conclusions

We have shown that the activity and selectivity of transition metal catalysts are strongly affected by the presence of metal oxide moieties on their surface. For polar reactants (e.g., CO, NO, $(CH_3)_2CO$) significant increases in the rate of reaction are observed. These are attributable to Lewis acid–base interactions between the one of the atoms in the dipole, i.e., O, and the metal cations exposed at the perimeter of the oxide moieties. The higher the Lewis acidity of the metal cations, the more effective it is as a promoter. Maximum promoter effectiveness is observed when the metal surface is covered by half a monolayer of the oxide, since in such cases the concentration of oxide perimeter sites is a maximum.

Acknowledgements

This work was supported by the Director, Office of Energy Research, Office of Basic Energy Sciences, Chemical Sciences Division of the US

Department of Energy under Contract DE-AC03-SF00098.

References

[1] S.J. Tauster, Acc. Chem. Res., 20 (1987) 389.
[2] A.T. Bell, in L.L. Hegedus, (Ed.), Catalyst Desigr - Progress and Perspectives, Wiley, New York, 1987.
[3] R. Burch, in Z. Paal and P.G. Menon, (Eds.), Hydrogen Effects in Catalysis, Marcel Dekker, New York, 1988.
[4] G.L. Haller and D.E. Resasco, Adv. Catal., 36 (1989) 173.
[5] M.A. Vannice, J. Mol. Catal., 59 (1990) 165; Catal. Today, 12 (1992) 255.
[6] G.-M. Schwab, Adv. Catal., 27 (1978) 1.
[7] F. Solymosi, Catal. Rev., 1 (1967) 233.
[8] R. Burch and A.R. Flambard, J. Catal., 86 (1982) 384.
[9] W.M.H. Sachtler and M. Ichikawa, J. Phys. Chem., 90 (1986) 4752.
[10] W.M.H. Sachtler, D.F. Shriver, W.B. Hollenberg and A.F. Lang, J. Catal., 92 (1985) 429.
[11] Y.-W. Chung, G. Xiong and C.C. Kao, J. Catal., 85 (1984) 237.
[12] R.A. Demmin, C.S. Ko and R.J. Gorte, J. Phys. Chem., 89 (1985) 1151.
[13] R.A. Demmin and R.J. Gorte, J. Catal., 98 (1986) 577.
[14] R.A. Demmin and R.J. Gorte, J. Catal., 105 (1987) 373.
[15] M.E. Levin, M. Salmeron, A.T. Bell and G.A. Somorjai., Surf. Sci.169 123 (1986).
[16] M.E. Levin, M. Salmeron, A.T. Bell and G.A. Somorjai., J. Chem. Soc., Faraday Trans. 1, 83 (1987) 2061.
[17] M.E. Levin, M. Salmeron, A.T. Bell and G.A. Somorjai., J. Catal., 106 (1987) 401.
[18] M.E. Levin, M. Salmeron, A.T. Bell and G.A. Somorjai., Surf. Sci.195 (1988) 429.
[19] K.J. Williams, M. Salmeron, A.T. Bell and G.A. Somorjai, Surf. Sci.204 (1988) L745.
[20] K.J. Williams, A.B. Boffa, M. Salmeron, A.T. Bell and G.A. Somorjai., Catal. Lett., 5 (1990) 385.
[21] K.J. Williams, A.B. Boffa, M. Salmeron, A.T. Bell and G.A., Somorjai., Catal. Lett., 9 (1991) 41.
[22] A.B. Boffa, A.T. Bell and G.A. Somorjai, J. Catal., 139 (1993) 602.
[23] A.B. Boffa, C. Lin, A.T. Bell and G.A. Somorjai, J. Catal., 149 (1994) 149.
[24] A.B. Boffa, C. Lin, A.T. Bell and G.A. Somorjai, Catal. Lett., 27 (1994) 243.
[25] K.J. Williams, M.E. Levin, M. Salmeron, A.T. Bell and G.A. Somorjai, A.C.S. Symp. Ser., 411 (1989) 183.
[26] A.B. Boffa, H.C. Galloway, P.W. Jacobs, J.J. Benitez, J.D. Batteas, M. Salmeron, A.T. Bell and G.A. Somorjai, Surf. Sci., 326 (1995) 80.
[27] T. Mori, H. Masuda, H. Imai, A. Miyamoto, R. Hasabe and Y. Murakami, J. Phys. Chem., 87 (1983) 3648.
[28] T. Mori, A. Miyamoto, N. Niizuma, N. Takahashi, T. Hattori and Y. Murakami, J. Phys. Chem., 90 (1986) 109.
[29] Y. Mori, T. Mori, A. Miyamoto, N. Takahashi, T. Hattori and Y. Murakami, J. Phys. Chem., 93 (1989) 2039.
[30] J.S. Rieck and A.T. Bell, J. Catal., 113 (1985) 341.
[31] E. Shustorovich and A.T. Bell, J. Catal., 96 (1985) 88.
[32] A. Amariglio, A. Elbiache and H. Amariglio, J. Catal., 98 (1986) 355.
[33] I. Fisher and A.T. Bell, unpublished results.
[34] K. Tanabe, Solid Acids and Bases, Kondansha, Tokyo and Academic Press, New York, 1970.
[35] K. Tanabe, in M. Boudart and J. Anderson (Eds.), Catalysis – Science and Technology, Vol. 2, Springer Verlag, Berlin, 1981
[36] K.I. Tanaka and A. Ozaki, J. Catal., 8 (1967) 1.
[37] R.T. Sanderson, Chemical Periodicity, Reinhold, New York, 1960.
[38] T. Iizuka, Y. Tanaka and K. Tanabe, J. Catal., 76 (1982) 1.
[39] T. Iizuka, Y. Tanaka and K. Tanabe, J. Mol. Catal., 17 (1982) 381.
[40] H.C. Wang, D.F. Ogletree and M. Salmeron, J. Vac. Sci. Tech. A,, 9 (1991) 853.
[41] T. Komaya, A.T. Bell, Z. Weng-Sieh, R. Gronsky, F. Engelke, T.S. King and M. Pruski, J. Catal., 149 (1994) 142.
[42] T. Komaya, A.T. Bell, Z. Weng-Sieh, R. Gronsky, F. Engelke, T.S. King and M. Pruski, J. Catal., 150 (1994) 400.
[43] T. Komaya, A.T. Bell, Z. Weng-Sieh, R. Gronsky, F. Engelke, T.S. King and M. Pruski, J. Catal., 152 (1995) 350.
[44] X. Wu, B.C. Gerstein and T.S. King, J. Catal., 118 (1989) 238.
[45] (a) S. Bhatia, F. Engelke, M. Pruski, B.C. Gerstein and T.S. King, J. Catal.,, 147 (1994) 455; (b) F. Engelke, S. Bhatia, T.S. King and M. Pruski, Phys. Rev. B, 49 (1994) 2730.
[46] A.K. Singh, N.K. Pande and A.T. Bell, J. Catal., 94 (1985) 422.
[47] A.K. Datye and D.J. Smith, Catal. Rev. Sci. Eng., 34 (1992) 129.
[48] M.A. Vannice and B. Sen, J. Catal., 115 (1989) 65.
[49] B. Sen and M.A. Vannice, J. Catal., 113 (1988) 52.
[50] S.D. Lin, D.K. Sanders and M.A. Vannice, Appl. Catal. A, 113 (1994) 59; J. Catal., 147 (1994) 375.
[51] K.J. Williams, A.B. Boffa, J. Lahtinen, M. Salmeron, A.T. Bell and G. A. Somorjai, Catal. Lett., 5 (1990) 385.
[52] K.J. Williams, A.B. Boffa, M. Salmeron, A.T. Bell and G.A. Somorjai, Catal. Lett., 11 (1991) 77.
[53] M. Ichikawa, A.J. Lang, D.F. Shriver and W.M.H. Sachtler, J. Am. Chem. Soc., 107 (1985) 7216.
[54] N.T. Pande and A.T. Bell, J. Catal., 98 (1986) 577.
[55] K.J. Williams, M. Salmeron, A.T. Bell and G.A. Somorjai, Catal. Lett., 1 (1988) 331.